Jurnal Teknologi

Full Paper

INPUT SHAPING TECHNIQUES FOR SWAY CONTROL OF A ROTARY CRANE SYSTEM

Ahmad Alhassan[a], Z. Mohamed[a*], Auwalu M. Abdullahi[b], Amir A. Bature[b], Ado Haruna[a,b], Nura M. Tahir[a]

[a]Faculty of Electrical Engineering, Universiti Teknologi Malaysia, 81310 UTM Johor Bahru, Johor, Malaysia
[b]Department of Mechatronics Engineering, Bayero University, Kano, Nigeria

Article history
Received
29 December 2016
Received in revised form
12 July 2017
Accepted
1 November 2017

*Corresponding author
zahar@fke.utm.my

Graphical abstract

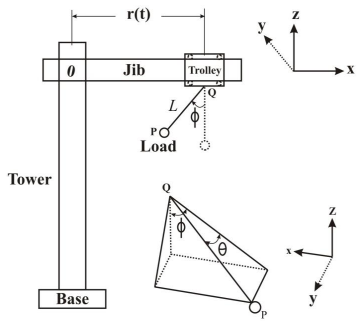

Abstract

This paper investigates the performance of input shaping techniques for sway control of a rotary crane system. Unlike the conventional optimal controllers, input shaping is simple to design and cost effective as it does not require feedback sensors. Several input shapers were implemented and their performances were compared which are useful for future sway control designs. A nonlinear model of the system was derived using the Lagrange's equation. To investigate the performance and robustness of input shaping techniques, zero vibration (ZV), zero vibration derivative (ZVD), zero vibration derivative-derivative (ZVDD) and zero vibration derivative-derivative-derivative (ZVDDD) were proposed with a constant cable length. Level of reduction of the payload sway is used to assess the control performance of the shapers. Simulation and real time experimental results have shown that ZVDDD with a sway reduction of 88% has the highest level of sway reduction and highest robustness to modeling errors as compared to other shapers.

Keywords: Rotary crane, Lagrange, input shaping, simulation, real time experiment, sway control

Abstrak

Kertas ini mengkaji prestasi teknik pembentukan masukan untuk kawalan ayunan sistem kren berputar. Tidak seperti pengawal optima yang konvensional, pembentukan masukan ringkas untuk di reka bentuk dan efektif dari segi kos dimana ianya tidak memerlukan pengesan suap balik (*feedback*). Beberapa pembentuk masukan dilaksanakan dan prestasinya telah dibandingkan, dimana ianya berguna untuk mereka bentuk pengawal ayunan pada masa akan datang. Satu model tidak linear dari sistem telah diterbitkan menggunakan persamaan Lagrange. Untuk menyiasat prestasi dan keteguhan teknik pembentukan masukan, getaran sifar (ZV), terbitan getaran sifar (ZVD), terbitan-terbitan getaran sifar (ZVDD) dan terbitan-terbitan-terbitan getaran sifar (ZVDDD) telah dikemukakan dengan panjang kabel yang malar. Tahap pengurangan ayunan muatan digunakan untuk menilai prestasi kawalan pembentuk tersebut. Keputusan dari simulasi dan eksperimen masa nyata telah membuktikan bahawa ZVDDD telah menghasilkan pengurangan ayunan tertinggi sebanyak 88% dan keteguhan tertinggu berbanding dengan teknik pembentukan masukan lain.

Kata kunci: Kren berputar, Lagrange, membentuk input, simulasi, percubaan, bergoyang kawalan

1.0 INTRODUCTION

Rotary cranes are commonly used tools in construction sites, mining industries, shipping industries and factories for conveyance, loading and unloading different items from one point to another. Due to their flexibility and wide operating range, they are also employed in hazardous environment. A rotary crane consists of a fixed tower, a rotating jib and a movable trolley which carries the load using a hoisting cable. During an operation, cranes suffer from an undesirable deflection and swinging of the payload which affects the performance of the system immensely. These oscillations could be higher with the presence of external forces such as rain and wind. It leads to a difficult positioning of the payload, delay in task completion and a high maintenance cost [1-5].

There have been numerous efforts by many researchers to minimize these persistent oscillations for a reliable and efficient operation of rotary crane systems. Varieties of open-loop and closed-loop controls ranging from a simple Proportional-Integral-Derivative (PID) control to intelligence control have been presented. In [6], an open-loop control was proposed by considering a horizontal boom motion of a rotary crane only. Performances of a feed-forward input shaping and a low pass filtering (LPF) have been investigated in [7]. It was observed that input shaping was more robust as compared to LPF for an erroneous natural frequency. Singer and Seering [8] were the first to propose a practically applicable input shaping scheme and since then it has been applied to various flexible structures. Using this technique, a zero oscillatory response can be achieved. Induced vibration of a flexible robot manipulator has been reduced using command shaping [9]. The sensitivity of zero vibration (ZV), zero vibration derivative (ZVD) and zero vibration derivative-derivative (ZVDD) shapers to errors of natural frequencies has been analyzed using a flexible beam in [3]. Input shaping has also been applied to other types of crane systems in [10-14]. However, open loop controllers are prone to external disturbances [15]. Though, an efficient control can be achieved by using open loop control in conjunction with feedback control [16].

In addition, straight transfer transformation method has been implemented for an optimal control of a rotary crane in [17]. A partial feedback linearization (PFL) and adaptive sliding mode control (SMC) for sway suppression of a rotary crane in a situation of inaccurate model or poor parameter representation has been presented in [18]. Although simple to design and implement, PFL is highly affected by a parameter variation such as cable length. A robust controller, SMC has been applied to other cranes [19, 20]. However, SMC has a drawback due to the fact that it dissipates a lot of energy which leads to a system burn-out (chattering) [21]. A three layered neural network with a genetic algorithm has been presented in [22], for vibration control of rotary crane. Besides, a comparison of optimal and intelligent sway control for a lab-scale rotary crane has been presented in [23]. A combined fuzzy logic and a delayed feedback controller for oscillation reduction of a rotary crane have been presented in [5]. Various intelligent controllers have also been proposed for other types of cranes in [24]. Besides, an improved input shaper [25], input-shaping with a distributed delay [26], input shaping techniques for anti-sway control [27] and a command shaping based on system output [13,14] have been proposed for crane systems. However, due to the highly nonlinear behavior and lack of standard linear model of the rotary cranes, most of the existing literature on the input shaping and other control methods focus on the sway control of gantry crane and overhead 3D cranes.

This paper presents a performance comparison of positive input shapers namely ZV, ZVD, ZVDD and zero vibration derivative-derivative-derivative (ZVDDD) for payload sway control of a rotary crane. The work gives an in-depth analysis of the behavior of the rotary cranes both using simulations and real-time experiment. In addition, the results will be useful as the feed-forward controller can be combined with a feedback controller for an efficient sway and position control. The input shapers were simulated with a nonlinear dynamic model of the crane using MATLAB. A laboratory tower crane was used experimentally to verify the effectiveness of the proposed shapers. Due to its highly nonlinearity and numerous outputs, sway of the payload for cart motion along the horizontal jib is considered.

2.0 METHODOLOGY

The work involves modelling of the rotary crane and development of several input shaping control techniques.

2.1 Modeling of a Rotary Crane

This section presents the description and mathematical modeling of a rotary crane. Figure 1 shows the laboratory rotary crane model. The schematic diagram of the rotary crane is shown in Figure 2. The structure consists of the followings:

1) A base that supports the overall structure. It is normally fixed to the ground to prevent unwanted vibration.
2) A tower that supports the jib. It is responsible for the rotational motion of the jib.
3) A jib that is connected to the tower and rotates the load horizontally about the fixed tower.
4) A cart that carries the load and slides along the jib.

Therefore, the rotary crane can operated by moving the load from one point to another with the added flexibility of rotational motions. Thus, the combined motion can place the load at any point within the reach of the crane. In order to avoid an obstacle, the suspension cable is manipulated using a

process called hoisting, to lift or lower the load. For the derivation of the nonlinear model of the rotary crane, a reference point *O* is set at the intersection of the fixed tower with the horizontal jib as shown in Figures 1 and 2. A right handed Cartesian coordinate (xyz) is centered at the reference point. The jib rotates horizontally at an angle $\gamma(t)$ around z-axis. The cart slides along the jib for a distance *r(t)* measured from the reference point to the point of payload suspension. During the operation, the oscillation of the payload is characterized by two angles, ϕ and θ. The angle ϕ is the in-phase angle due to the translational motion of the cart known as x-angle while θ is the out-of-phase angle due to the rotation of the crane. It is also known as the *y*-angle. *L* is the length of the hoisting cable and *m* is the mass of the load and *g* is the gravitational acceleration. In this study, a metallic Inteco tower crane of dimension 1600 mm x 1200 mm, *L* = 0.6 m and *m* = 800 g is considered.

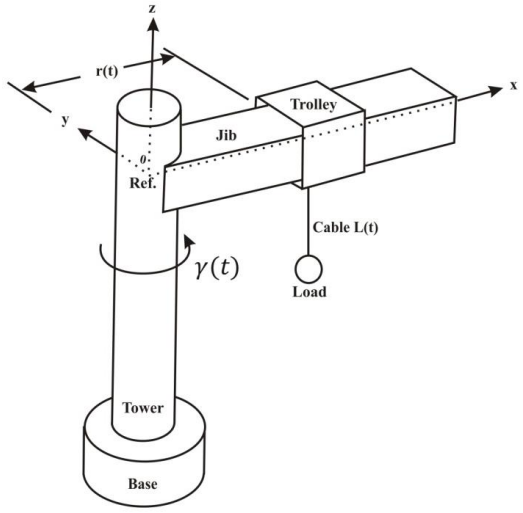

Figure 1 Rotary crane system

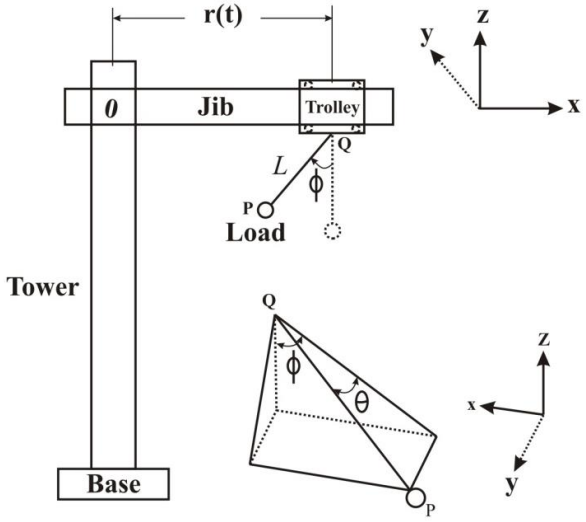

Figure 2 Schematic diagram of a rotary crane system

To reduce the complexity of modeling, the following assumptions were made.

1) The length of suspension cable is constant.
2) The trolley motion and jib rotation are frictionless.
3) External disturbance such as wind is neglected.

To derive the dynamic model, Lagrange's equation is utilized.

$$\frac{d}{dt}\left(\frac{\partial L}{\partial \dot{q}_i}\right)-\frac{\partial L}{\partial q_i}=Q_i,\ i=1,2,\ldots,n \tag{1}$$

where

$$L = K_E - P_E \tag{2}$$

K_E and P_E are respectively the total potential and kinetic energies, *n* is total number of independent generalized coordinate and Q_i is non-conservative generalized forces.

The velocity (ψ) and acceleration (γ) of the cart in xyz plane are given as

$$\psi = \dot{\gamma} \tag{3}$$

To find the position of the payload, *P(t)* with respect to the reference point *O*, *i*, *j*, *k* unit vectors are assigned. Thus,

$$\begin{aligned} P(t) = {} & [r(t) - L(t)cos\theta(t)\sin\phi(t)]i \\ & + [L(t)sin\theta(t)]j \\ & - [L(t)cos\theta(t)cos\phi(t)]k \end{aligned} \tag{4}$$

The combined velocity of the payload ($\dot{P}(t)$) is

$$\dot{P}(t) = \frac{\delta P(t)}{\delta(t)} + \psi(t)P(t) \tag{5}$$

The kinetic energy of the load can be obtained as

$$K_E = \frac{1}{2}m[\dot{P}(t)\dot{P}(t)] \tag{6}$$

On the other hand, the potential energy of the load is given as

$$P_E = -mgL(t)cos\theta(t)cos\phi(t) \tag{7}$$

Solving for Equation (2) and substituting for $q_1 = \theta$ and $q_2 = \phi$ in Equation (1) gives the nonlinear differential equations as

$$\begin{aligned}\ddot{\theta}(t) - 2\dot{\gamma}(t)cos\phi(t)cos^2\theta(t)\dot{\phi}(t) + \frac{1}{2}sin2\theta(t)\dot{\phi}^2(t) \\ -\frac{1}{2}\dot{\gamma}^2(t)sin2\theta(t)cos^2\phi(t) \\ +\frac{g}{L}sin\theta(t)cos\phi(t) \\ +\frac{2}{L}\dot{r}(t)\dot{\gamma}(t)cos\theta(t) \\ -+\frac{1}{L}r(t)\dot{\gamma}^2(t)sin\theta(t)sin\phi(t) \\ +\frac{1}{L}\ddot{r}(t)sin\theta(t)sin\phi(t) \\ +\frac{1}{L}r(t)\ddot{\gamma}(t)cos\theta(t) - \ddot{\gamma}(t)sin\phi(t) \\ = 0\end{aligned} \tag{8}$$

$$\begin{aligned}cos\theta(t)(t)\ddot{\phi}(t) + 2\dot{\gamma}(t)cos\theta cos\phi(t)\dot{\theta}(t) \\ -2sin\theta(t)\dot{\theta}(t)\dot{\phi}(t) + \frac{g}{L}sin\phi(t) \\ +cos\phi(t)\dot{\gamma}^2(t)\left\{\frac{1}{L}r(t)\right. \\ \left.-sin\phi(t)cos\theta(t)\right\} \\ +\ddot{\gamma}(t)sin\theta(t)cos\phi(t) \\ -\frac{1}{L}\ddot{r}(t)cos\phi(t) = 0\end{aligned} \tag{9}$$

2.2 Control Design

This section describes the development of the input shapers for the payload sway. The shapers are ZV, ZVD, ZVDD and ZVDDD. In addition, a logarithmic decrement approach for the estimation of the natural frequency and damping ratio of the system is also presented.

2.2.1 Input Shaping Technique

As discussed earlier, a shaped input is obtained by convolving the reference input with a sequence of impulses. The impulse amplitudes and their respective time instants constitute the shaper's parameter [28]. Natural frequency and damping ratio are used to determine those parameters. The objective is to determine the appropriate parameters which will drive the system with zero oscillatory response. Figure 3 shows the simplest input shaping process containing two impulses (ZV). The response of a rotary crane can be considered as a second order underdamped system of the form

$$G(s) = \frac{\omega^2}{s^2 + 2\omega\zeta + \omega^2} \tag{10}$$

where ω is the natural frequency and ζ is the damping ratio of the system in time domain. The response of the system can be expressed as

$$\begin{aligned}y(t) = \frac{A\omega}{\sqrt{(1-\zeta^2)}}e^{-\zeta\omega(t-t_0)}sin\left(\omega(t\right. \\ \left.-t_0)\sqrt{(1-\zeta^2)}\right)\end{aligned} \tag{11}$$

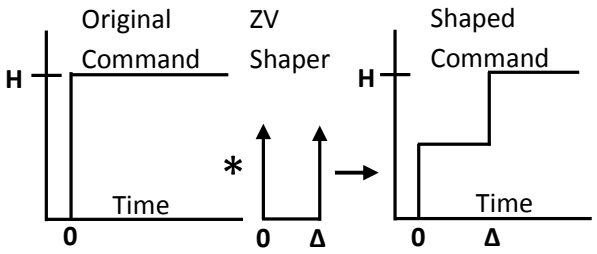

Figure 3 Input shaping process

where A and t_0 are the amplitude and time instant of the impulse, respectively. By superposition, the response to an impulses sequence after the last impulse can be obtained as

$$\begin{aligned}y(t) = \sum_{i=0}^{n}\left[\frac{A\omega}{\sqrt{(1-\zeta^2)}}e^{-\zeta\omega(t-t_0)}\right]sin\left(\omega(t\right. \\ \left.-t_0)\sqrt{(1-\zeta^2)}\right)\end{aligned} \tag{12}$$

The amplitude of the residual vibration can be determined by using the trigonometric function.

$$\sum_{i=0}^{n} B_i\, sin(\omega t + \beta_i) = Asin(\omega t - \varphi) \tag{13}$$

where

$$A = \sqrt{\left(\sum_{i=0}^{n} B_i\, cos(\beta_i)\right)^2 + \left(\sum_{i=0}^{n} B_i\, cos(\beta_i)\right)^2} \tag{14}$$

By comparing Equations (12) and (13) yields

$$B_i = \frac{A_i\omega_n}{\sqrt{(1-\zeta^2)}}e^{-\zeta\omega(t-t_i)} \tag{15}$$

To calculate the residual oscillation amplitude, Equation (15) is evaluated at the last impulse, $t = t_n$. By substituting Equation (15) into Equation (14) and taking the constant part of the coefficients out of the square roots gives

$$A = \frac{\omega}{\sqrt{(1-\zeta^2)}}e^{-\zeta\omega t_n}\sqrt{{R_1}^2 + {R_2}^2} \tag{16}$$

where

$$\begin{aligned}R_1 = \sum_{i=0}^{n} A_i e^{\zeta\omega t_i} sin\left(\omega t_i\sqrt{(1-\zeta^2)}\right) \\ R_2 = \sum_{i=0}^{n} A_i e^{\zeta\omega t_i} cos\left(\omega t_i\sqrt{(1-\zeta^2)}\right)\end{aligned} \tag{17}$$

The expression for the non-dimensional function of the vibration amplitude can be obtained by dividing

Equation (16) by the residual vibration of the single impulse of unity magnitude. The residual oscillation amplitude from a unity magnitude at $t = 0$ can be obtained as

$$A_{\uparrow} = \frac{\omega}{\sqrt{(1-\zeta^2)}} \tag{18}$$

Hence, by dividing Equation (16) and Equation (18) gives the percentage residual vibration as

$$R = \frac{A}{A_{\uparrow}} = e^{-\zeta\omega t_n}\sqrt{{R_1}^2 + {R_2}^2} \tag{19}$$

To obtain zero vibration after the last impulse, both R_1 and R_2 of Equation (19) should set to zero independently. This is called zero vibration (ZV) constraint. To obtain a similar rigid body motion of unshaped command, the sum of the shaper's amplitudes of the impulse should be unity. This gives the summation constraints as

$$\sum_{i=1}^{n} A_i = 1 \tag{20}$$

In addition, to avoid unnecessary response delay, the time instants of the first impulse is set at $t_1 = 0$. Therefore, to design a ZV shaper, two impulse sequences are considered. Thus, solving for Equations (19) and (20) using the ZV constraints yields the ZV parameters as

$$\begin{pmatrix} A_i \\ t_i \end{pmatrix} = \begin{pmatrix} \frac{1}{1+k} & \frac{k}{1+k} \\ o & \tau_d \end{pmatrix} \tag{21}$$

where

$$\tau_d = \frac{\pi}{\omega\sqrt{(1-\zeta^2)}} \;\; ; \;\; k = e^{\frac{-\zeta\pi}{\sqrt{(1-\zeta^2)}}} \tag{22}$$

However, the ZV shaper does not account for robustness to frequency errors. This robustness can be increased by setting the derivatives of both R_1 and R_2 to zero which will produce small changes in vibration in proportion to the frequency errors. In general, the derivative of the residual vibration can take the form of

$$\frac{\delta^i R_1}{\delta\omega^i} = 0 \;\; ; \;\; \frac{\delta^i R_2}{\delta\omega^i} = 0 \tag{23}$$

The shapers can also take the form of ZV(D)^i, with $i \geq 0$ as the derivate order. To design ZVD, first derivative of R_1 and R_2 is considered i.e $i = 1$. Thus, solving the constraints equations of Equation (19), (20) and (23) gives the three impulse ZVD shaper's parameters as

$$\begin{pmatrix} A_i \\ t_i \end{pmatrix} = \begin{pmatrix} \frac{1}{(1+k)^2} & \frac{2k}{(1+k)^2} & \frac{k^2}{(1+k)^2} \\ o & \tau_d & 2\tau_d \end{pmatrix} \tag{24}$$

In addition, to design ZVDD, second derivative is considered i.e $i = 2$. Thus, solving the constraints in Equations (19), (20) and (23) gives the four impulse ZVDD shaper's parameters as

$$\begin{pmatrix} A_i \\ t_i \end{pmatrix} = \begin{pmatrix} \frac{1}{(1+k)^3} & \frac{3k}{(1+k)^3} & \frac{3k^2}{(1+k)^3} & \frac{k^3}{(1+k)^3} \\ o & \tau_d & 2\tau_d & 3\tau_d \end{pmatrix} \tag{25}$$

Using the similar approach, for $i = 3$, the five impulse ZVDDD shaper's parameters can be obtained as

$$\begin{pmatrix} A_i \\ t_i \end{pmatrix} = \begin{pmatrix} \frac{1}{(m)^4} & \frac{4k}{(m)^4} & \frac{6k^2}{(m)^4} & \frac{4k^3}{(m)^4} & \frac{k^4}{(m)^4} \\ o & \tau_d & 2\tau_d & 3\tau_d & 4\tau_d \end{pmatrix} \tag{26}$$

where $m = 1 + k$.

2.2.2 Finding Natural Frequency and Damping Ratio

The most important parameters for the design of any input shaper are the natural frequency and damping ratio of the system. In this study, a logarithmic decrement approach is employed as described in [3, 29]. Consider the response of an underdamped system as in Figure 4. For a decaying free damped system, a logarithmic decrement approach is the effective and simplest technique to determine the natural frequency and damping ratio directly from the time response curve. To estimate the damping ratio of this system, any two successive peaks can be selected given as

$$\zeta = \frac{\ln(\frac{y_1}{y_2})}{\sqrt{4\pi^2 + \left(\ln(\frac{y_1}{y_2})\right)^2}} \;\; ; \;\; \omega = \frac{\ln(\frac{y_1}{y_2})}{\zeta(t_2 - t_1)} \tag{27}$$

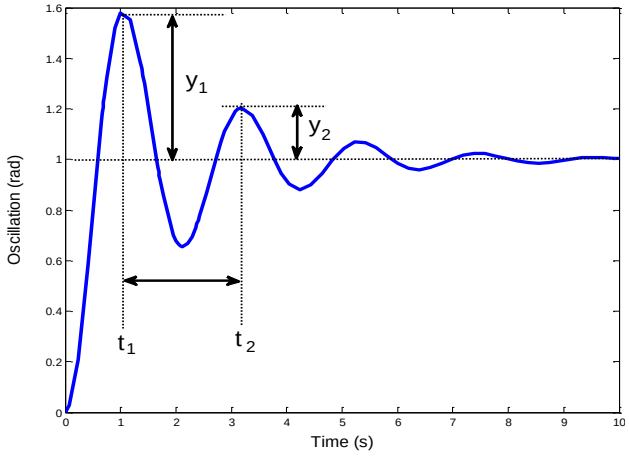

Figure 4 Logarithmic decrement approach

2.2.3 Mean-Absolute-Error (MAE)

In this paper, the mean absolute error (MAE) is used for the performance assessment. The MAE is the most natural measure of average error for performance

analysis of sway reduction. The mathematical expression is given as

$$MAE = \frac{\sum_{i=1}^{n}|y_i - x_i|}{n} \quad (28)$$

where *n* is the number of plot points, x_i and y_i are the i^{th} point coordinates respectively.

2.3 Input Shaping for the Rotary Crane

In order to study the dynamics of the system, a pulse input torque as shown in Figure 5 is applied to the nonlinear model of Equations (8) and (9). This input is sufficient to cause the system to move and then stop, resulting to an oscillatory response of the load.

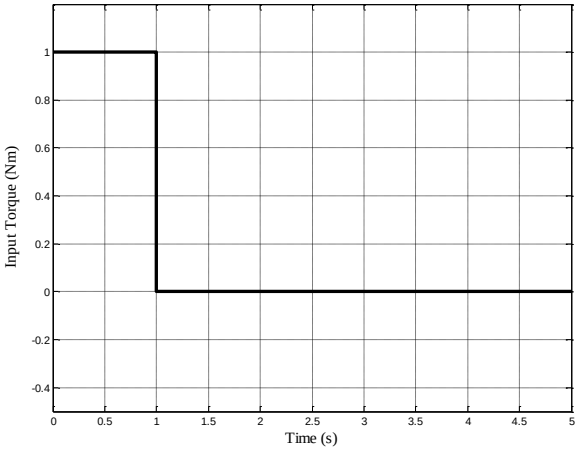

Figure 5 Pulse input signal

Using the logarithmic decrement approach of Figure 4, the natural frequency and damping ratio of the system were respectively calculated as 3.8080 rad/s and 0.0012. By using the estimated natural frequency and damping ratio, and solving Equations (21), (24), (25) and (26), the parameters of ZV, ZVD, ZVDD and ZVDDD can be calculated. Table 1 shows the designed shapers parameters from the system response. The designed shapers were applied to the rotary crane as a feedforward controllers as shown in Figure 6. A payload sway response is monitored and analyzed in time domain.

Table 1 Input shaping control parameters

Shaper	ZV	ZVD	ZVDD	ZVDDD
A_1	0.5010	0.2510	0.1257	0.0630
A_2	0.4990	0.5000	0.3757	0.2510
A_3	-	0.2490	0.3743	0.3750
A_4	-	-	0.1243	0.2490
A_5	-	-	-	0.0620
t_1 (s)	0	0	0	0
t_2 (s)	0.8250	0.8250	0.8250	0.8250
t_3 (s)	-	1.6500	1.6500	1.6500
t_4 (s)	-	-	2.4750	2.4750
t_5 (s)	-	-	-	3.3000

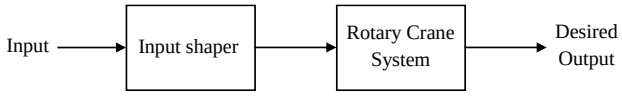

Figure 6 Input shaping block diagram for the rotary crane

3.0 RESULTS AND DISCUSSION

In this section, simulation and experimental results of the designed input shapers is presented and discussed. To investigate the performance of the designed shapers, level of sway reduction has been used. This is achieved by comparing the MAE of the unshaped and shaped responses.

3.1 Simulation Results

Simulation results of the response of the rotary crane subjected to an unshaped and shaped input command is shown in Figure 7. The MAE values of the unshaped, ZV, ZVD, ZVDD and ZVDDD are 0.0563 rad, 0.0105 rad, 0.0082 rad, 0.0072 rad and 0.0063 rad respectively. These represent 81.35%, 85.44%, 87.21% and 88.81% of sway reduction by the respective shapers as compared to the unshaped input.

To investigate the robustness of the proposed shapers to modeling error, the natural frequency of the system was increased and decreased by 25% of the actual value. Figures 8 and 9 show the response with an erroneous natural frequency. The MAE values for response for the exact, increased and decreased natural frequency is shown in Figure 10. Investigation of the time response characteristics in terms of rise time and settling time show that ZVDDD is much slower than ZV shaper. This is due to the number of additional delays. In such case, ZVDDD has the slowest response time whereas ZV has the fastest response. Thus, the higher the derivatives order of the residual vibration, the slower the response of the system.

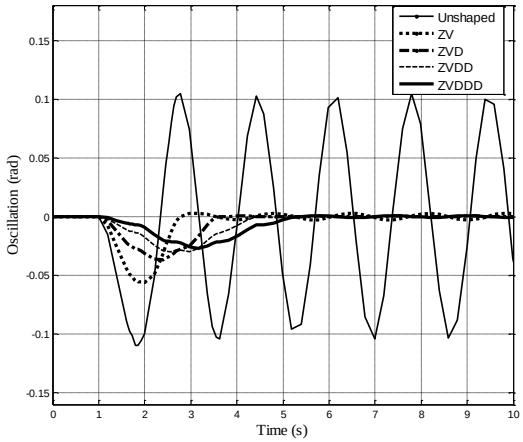

Figure 7 Unshaped and shaped responses for exact frequency

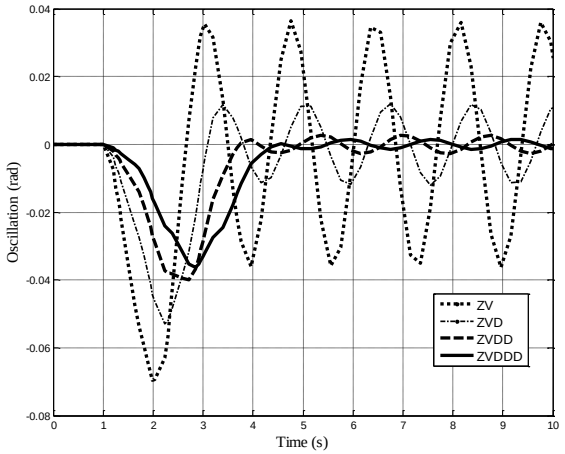

Figure 8 Shaped responses for 25% increase of frequency

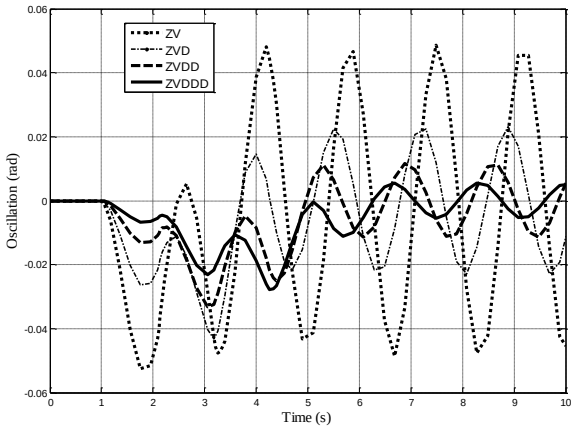

Figure 9 Shaped responses for 25% decrease of frequency

The summary of the corresponding MAE values are tabulated in terms of percentages of the sway reduction as shown in Table 2.

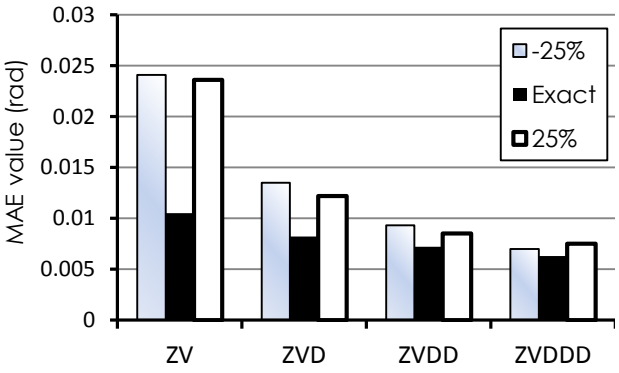

Figure 10 MAE values for the exact and erroneous frequency

Table 2 Level of sway reduction (simulation)

Shaper	Percentage of sway reduction		
	-25% ω	Exact ω	+25% ω
ZV	57.20%	81.35%	58.08%
ZVD	76.02%	85.44%	78.33%
ZVDD	83.48%	87.21%	84.90%
ZVDDD	87.57%	88.81%	86.68%

3.2 Experimental Results

Experimental results of using the input shapers are presented in this section for validation of the simulated results. A laboratory rotary crane setup as shown in Figure 11 is utilized for the validation. The hardware and its supporting components were controlled from MATLAB environment using installed rotary crane graphical user interface (GUI) via RT-DAC/PCI-D I/O board. The motors allowed the motion of the trolley along the jib as well as the rotation of the tower. The encoders sense the position of the trolley and the corresponding sway of the payload.

The setup was energized with the same pulse input signal of Figure 5. This causes the cart to move and then stop resulting to the suspended payload to oscillate. The same input shaper parameters of Table 1 were used in this experiment. Figure 12 shows the results obtained from the open loop test compared with the proposed shapers. Similarly, to investigate the robustness modeling errors of the implemented shapers, the natural frequency of the system was deliberately increased by 25% of the actual value as shown in Figure 13. The MAE values of each shaper are compared in Figure 14. The comparison for percentage of sway reduction by the designed shapers based on MAE of the responses is shown in Table 3. This confirmed that ZVDD and ZVDD are not significantly affected by errors in modeling frequency. Interestingly, the simulation and experimental results approximately gave similar results for all the shapers as shown in Figure 15.

Figure 11 A laboratory rotary crane

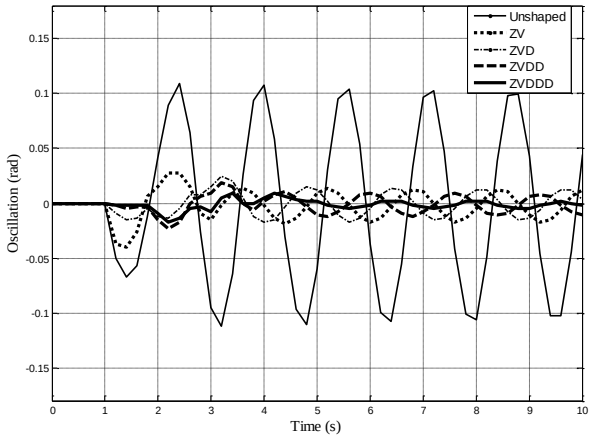

Figure 12 Unshaped and shaped responses for exact natural frequency

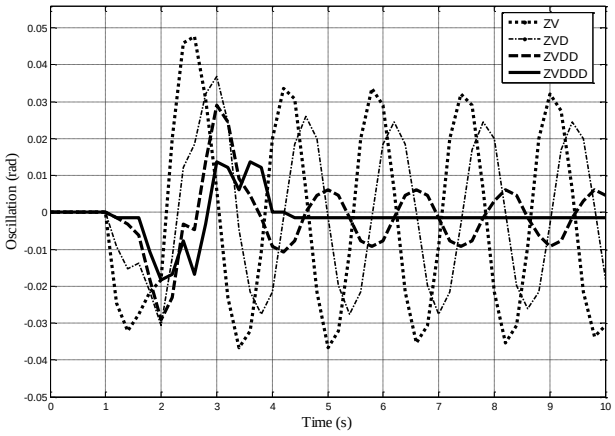

Figure 13 Shaped responses for 25% increase of frequency

Table 3 Level of sway reduction (experiment)

Shaper	Percentage of sway reduction		
	-25% ω	Exact ω	+25% ω
ZV	57.20%	81.35%	58.08%
ZVD	76.02%	85.44%	78.33%
ZVDD	83.48%	87.21%	84.90%
ZVDDD	87.57%	88.81%	86.68%

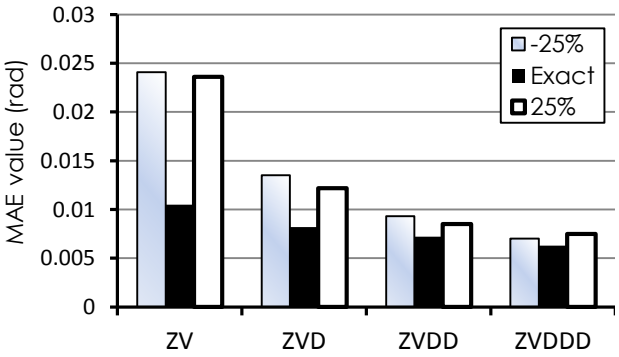

Figure 14 MAE value for exact and erroneous frequency

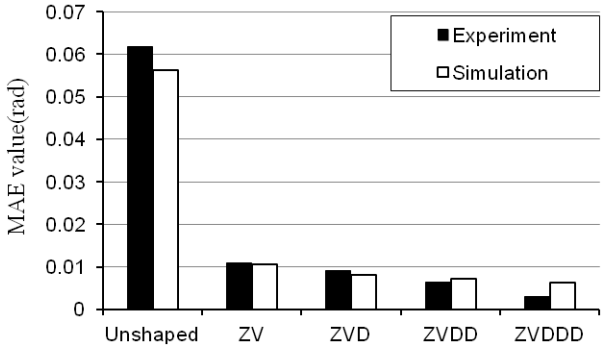

Figure 15 MAE value for shaped and unshaped results for simulation and experiment

4.0 CONCLUSION

Investigations into sway control schemes for a rotary crane system using four positive input shapers namely, ZV, ZVD, ZVDD and ZVDDD have been presented. Simulations using a nonlinear model and experiments on a laboratory tower crane have been performed to study the effectiveness of the controllers. The performances of the designed shapers were assessed in terms of level of sway reduction and robustness to modeling errors. MATLAB simulation and experimental results of the proposed shapers showed a significant sway reduction of the payload was achieved using all the shapers. The performances of the shapers demonstrated that ZVDDD provides higher sway reduction and robustness compared to ZVDD, ZVD and ZV. Conversely, ZVDDD has the slowest response due to the additional number of delays. It was noted that ZV has the fastest response as compared to the other shapers.

References

[1] Ramli, L., Mohamed, Z., Abdullahi, A. M., Jaafar, H. I. and Lazim, I. M. 2017. Control Strategies for Crane Systems: A Comprehensive Review. *Mechanical Systems and Signal Processing*. 95: 1-23

[2] Singhose, W. 2009. Command Shaping for Flexible Systems: A Review of the First 50 Years. *International Journal of Precision Engineering and Manufacturing.* 10(4): 153-168.

[3] Ha, M., and Kang, C. 2013. Experimental Analysis of Natural Frequency Error to Residual Vibration in ZV , ZVD , and ZVDD Shapers. *10th International Conference on Ubiquitous and Ambient Intelligence.* 195-199.

[4] Bartulovi, M., and Zu, G. 2014. Nonlinear Predictive Control of a Tower Crane Using Reference Shaping Approach. *16th International Power Electronics and Motion Control Conference and Exposition.* 872-876.

[5] Masoud, Z. N., Nayfeh, A. H. and Al-mousa, A. 2003. Delayed Position-Feedback Controller for the Reduction of Payload Pendulations of Rotary Cranes. *Journal of Vibration and Control.* 9: 257-277.

[6] Uchiyama, N., Huimin, O., and Shigenori, S. 2013. Simple Rotary Crane Dynamics Modeling and Open-Loop Control for Residual Load Sway Suppression by Only Horizontal Boom Motion. *Mechatronics.* 23(8): 1223-1236.

[7] Ahmad, M., R. Raja, M. Ramli, N. Zakaria, and N. Abd Ghani. 2009. Robust Feed-Forward Schemes for Anti-Sway

Control of Rotary Crane. *1st International Conference on Computational Intelligence, Modelling, and Simulation(CSSim)*. 17-22.
[8] Seering, N. C. and Singer, W. P. 1990. Preshaping Command Inputs to Reduce System Vibration. *Journal of Dynamic Systems, Measurement and Control*. 112: 76-82.
[9] Mohamed, Z., Chee, A. K., Mohd, H., Tokhi, M. O, Amin, S. H. M and Mamat, R. 2006. Techniques for Vibration Control of a Flexible Robot Manipulator. *Robotica.* 24 (4): 499-511.
[10] Maleki, E., and W., Singhose. 2010. Dynamics and Zero Vibration Input Shaping Control of a Small-Scale Boom Crane. *2010 American Control Conference.* 2296-2301.
[11] Auwalu M. A., Z. Mohamed, M. S. Zainal Abidin, R. Akmeliawati, A. R. Husain, A. A. Bature, A. Alhassan. 2015. Adaptive Input Shaping for Sway Control of 3D Crane using a Pole-Zero Cancellation Method. *IEEE Student Conference on Research and Development (SCOReD).* 1-6.
[12] Alhassan, A., K. A. Danapalasingam, M. Shehu, A. M. Abdullahi, and A. Shehu. 2015. Comparing the Performance of Sway Control Using ZV Input Shaper and LQR on Gantry Cranes. *9th Asia Modeling Symposium.* 61-66.
[13] Abdullahi, A. M., Mohamed, Z., Zainal Abidin, M. S., Buyamin, S. and Bature, A. A. 2017. Output-based Command Shaping Technique for an Effective Payload Sway Control of a 3D Crane with Hoisting. *Transactions of the Institute of Measurement and Control*. 39(10): 1443-1453.
[14] Abdullahi, A. M., Mohamed, Z., Pota, H. R., Selamat, H., Zainal Abidin, M. S., Ismail, F. S. and Haruna, A. 2018. Adaptive Output-based Command Shaping for Sway Control of an Overhead 3D Crane with Payload Hoisting in the Presence of Wind Disturbance. *Mechanical Systems and Signal Processing*. 98: 157-172.
[15] Vaughan, J., A. Yano, and W. Singhose. 2008. Performance Comparison of Robust Input Shapers. *American Control Conference.* 3257-3262.
[16] Schaper, U., E. Arnold, O. Sawodny, and K. Schneider. 2013. Constrained Real-Time Model-Predictive Reference Trajectory Planning for Rotary Cranes. *IEEE/ASME International Conference on Advanced Intelligent Mechatronics: Mechatronics for Human Wellbeing*. 680-685.
[17] Terashima, K., Ying, S., and Ken'ichi, Y. 2007. Modeling and Optimal Control of a Rotary Crane Using the Straight Transfer Transformation Method. *Control Engineering Practice.* 15 (9): 1179-1192.
[18] Le, T. A., Viet-hung, D., Deok, H. K., and Tran, N. 2012. Nonlinear Controls of a Rotating Tower Crane in Conjunction with Trolley Motion. *Systems and Control Engineering.* 227(5): 451-460.
[19] Bartolini, G., Alessandro, P., and Elio, U. 2002. Second-Order Sliding-Mode Control of Container Cranes. *Automatica.* 38(10): 1783-1790.
[20] Tuan, L., and Soon-geul, L. 2013. Sliding Mode Controls of Double-Pendulum Crane Systems. *Journal of Mechanical Science and Technology.* 27(6): 1863-1873.
[21] Tuan, L., Sang-chan, M., Won, G., and Soon-geul, L. 2013. Adaptive Sliding Mode Control of Overhead Cranes with Varying Cable Length. *Journal of Mechanical Science and Technology.* 27(3): 885-893.
[22] Nakazono, K., Kouhei, O., Hiroshi, K., and Tetsuhiko, Y. 2008. Vibration Control of Load for Rotary Crane System Using Neural Network with GA-Based Training. *Artificial Life and Robotics.* 13(1): 98-101.
[23] Ahmad, M., R. Samin, and M. Zawawi. 2010. Comparison of Optimal and Intelligent Sway Control for a Lab-Scale Rotary Crane System. *Second International Conference on Computer Engineering and Applications*. 229-234.
[24] Hyla, P. 2012. The Crane Control Systems : A Survey. *IEEE.* 505-509.
[25] Maghsoudi, M. J., Z. Mohamed, S. Sudin, S. Buyamin, H. I. Jaafar and S. M. Ahmad. 2017. An Improved Input Shaping Design for an Efficient Sway Control of a Nonlinear 3D Overhead Crane with Friction. *Mechanical Systems and Signal Processing*. 92: 364-378.
[26] Maghsoudi, M. J., Z. Mohamed, M. O Tokhi, A.R. Husain, and M. Z. Abidin. 2017. Control of a Gantry Crane Using Input-shaping Schemes with Distributed Delay. *Transactions of the Institute of Measurement and Control*. 39(3): 361-370.
[27] Maghsoudi, M. J., Z. Mohamed, A. R. Husain, and M. O. Tokhi. 2016. An Optimal Performance Control Scheme for a 3D Crane, *Mechanical Systems and Signal Processing*. 66-67: 756-768.
[28] Teo, C., Tan, K., Lim, S., Huang, S., and Tay, E. 2007. Dynamic Modeling and Adaptive Control of a H-Type Gantry Stage. *Mechatronics.* 17: 361-367.
[29] Pao, L. 1997. Analysis of the Frequency, Damping, and Total Insensitivities of Input Shaping Designs. *Journal of Guidance, Control, and Dynamics.* 20(5): 909-915.